Effect of Stimulus Waveform of Biphasic Current Pulse on Retinal Ganglion Cell Responses in Retinal Degeneration (*rd1*) mice

Kun No Ahn[1], Jeong Yeol Ahn[1], Jae-hyung Kim[2], Kyoungrok Cho[3], Kyo-in Koo[4], Solomon S. Senok[5], and Yong Sook Goo[1]

Departments of [1]Physiology and [2]Ophthalmology, Chungbuk National University School of Medicine, [3]Department of Information and Communication Engineering, Chungbuk National University College of Electrical and Computer Engineering, Cheongju 362-763, [4]Department of Electrical Engineering, University of Ulsan, Ulsan 680-749, Korea, [5]Devision of Neuroscience, Alfaisal University College of Medicine, Riyadh 11533, Kingdom of Saudi Arabia

A retinal prosthesis is being developed for the restoration of vision in patients with retinitis pigmentosa (RP) and age-related macular degeneration (AMD). Determining optimal electrical stimulation parameters for the prosthesis is one of the most important elements for the development of a viable retinal prosthesis. Here, we investigated the effects of different charge-balanced biphasic pulses with regard to their effectiveness in evoking retinal ganglion cell (RGC) responses. Retinal degeneration (*rd1*) mice were used (n=17). From the *ex-vivo* retinal preparation, retinal patches were placed ganglion cell layer down onto an 8×8 multielectrode array (MEA) and RGC responses were recorded while applying electrical stimuli. For asymmetric pulses, 1st phase of the pulse is the same with symmetric pulse but the amplitude of 2nd phase of the pulse is less than 10 μA and charge balanced condition is satisfied by lengthening the duration of the pulse. For intensities (or duration) modulation, duration (or amplitude) of the pulse was fixed to 500 μs (30 μA), changing the intensities (or duration) from 2 to 60 μA (60 to 1000 μs). RGCs were classified as response-positive when PSTH showed multiple (3∼4) peaks within 400 ms post stimulus and the number of spikes was at least 30% more than that for the immediate pre-stimulus 400 ms period. RGC responses were well modulated both with anodic and cathodic phase-1st biphasic pulses. Cathodic phase-1st pulses produced significantly better modulation of RGC activity than anodic phase-1st pulses regardless of symmetry of the pulse.

Key Words: Anodic phase-1st stimulus, Cathodic phase-1st stimulus, Multi-electrode array (MEA), Retinal ganglion cell (RGC), Retinal prosthesis

INTRODUCTION

The retina is a specialized organ for vision where the conversion of light energy into neural activity happens. Among many retinal diseases, retinitis pigmentosa (RP) and age-related macular degeneration (AMD) are leading causes of blindness in adults [1,2]. A variety of treatment modalities have been attempted to restore vision in these patients. Among them, retinal prosthesis is being developed and regarded as the most feasible method to restore vision [3-5].

While a lot of effort has been devoted to the development of electrodes, circuits, packaging, and surgical techniques [6], less attention has been paid to the electrical stimulation parameters that would permit reliable retinal stimulation. Finding optimal parameters for electrical stimulation is one of the most important elements for the development of a viable retinal prosthesis.

Due to the advantage of large number of recording and stimulation channels, multielectrode array (MEA) electrodes have been used to record from a wide variety of neuronal preparations including the isolated retina [7-13].

When designing electrical stimulation protocols, many things should be considered, even after deciding electrode, like whether to use voltage or current control, whether to use monopolar stimuli or bipolar stimuli, what pulse shapes to use (monophasic, biphasic, multiphasic or asymmetric), etc. The efficacy of the stimulus to evoke spikes and the safety of the stimulus to the electrode itself and tissue are

ABBREVIATIONS: ACSF, artificial cerebrospinal fluid; AMD, age-related macular degeneration; MEA, multielectrode array; OPL, outer plexiform layer; PSTH, post-stimulus time histogram; RGC, retinal ganglion cell; RP, retinitis pigmentosa; SD, strength-duration; TiN, titanium nitride.

issues that warrant careful consideration. Generally, the current stimulation method is preferred over the voltage stimulation method in the retinal prostheses because the current stimulation can accurately control the delivered amount of charge. The current stimulation, however, can generate quite high electrode voltages that may harm the tissues or damage the electrodes [14]. Several studies have shown that monophasic pulse stimuli are more tissue-damaging than charge-balanced biphasic pulses [15-19].

Therefore, we have investigated optimal electrical stimulation parameters for retinal prostheses. Previously, we used both voltage-controlled and current-controlled pulses and proposed the optimal stimulus range for normal retina (wild-type mice) and degenerated retina (*rd1*) mice [11]. In our previous study, we only used anodic phase-1st followed by cathodic phase-2nd pulse to satisfy charge balance [11]. There have been long debates on which pulse waveforms are better regarding efficacious spike initiation, tissue damage, corrosion, etc [20-22]. Understanding the response of retinal ganglion cells to different stimulus waveforms has potential clinical implications.

We report here the use of charge-balanced biphasic current pulse stimuli and compared the efficacy of anodic and cathodic phase-1st biphasic pulses on evoking RGC spikes from the *ex-vivo* retinal preparation of *rd1* mice, the well-established animal model of RP [23-25].

METHODS

Animals

Seventeen *rd1* (C3H/HeJ-*Pde6b^rd1^*) mice of postnatal 8~9 weeks were used for these experiments. At this postnatal age, the retinas are no longer responsive to light, but extensive remodeling of the inner retina has not yet occurred. Instead, functional stability of RGCs are well preserved up to postnatal day 210 [26]. All mice were purchased from the Jackson Laboratories (Bar Harbor, ME, USA) and were maintained on a 12 hour light/dark cycle. All experimental methods and animal care procedures were approved by the institutional animal care committee of Chungbuk National University (approval number: CBNURA-042-0902-1).

Retinal preparation

The *rd1* mice were anesthetized with an intraperitoneal injection of 1 ml/kg of a solution containing tiletamine-zolazepam hydroxide (25 mg/ml, Zoletil 50; Vervac, Sao Paulo, Brazil), xylazine hydrochloride (23.32 mg/ml, Rompun; Bayer Korea) and heparin sodium (5,000 I.U). After anesthesia, the retinal patches were prepared following the method of Stett et al. [8]. Briefly, the eye was enucleated, and then the retina was isolated and cut to patches of ~3×3 mm. The retinal patches were prepared under moderate illumination in an artificial cerebrospinal fluid (ACSF) solution (124 mM NaCl, 10 mM Glucose, 1.15 mM KH_2PO_4, 25 mM $NaHCO_3$, 1.15 mM $MgSO_4$, 2.5 mM $CaCl_2$ and 5 mM KCl) bubbled with 95% O_2+5% CO_2 to maintain a pH of 7.3~7.4 and a temperature of 32°C. Patches were then mounted onto a planar microelectrode array (MEA) ganglion cell layer down onto the MEA.

In-vitro MEA Recording system

The data acquisition system (MEA60 system; Multi Channel Systems GmbH, Reutlingen, Germany) included planar MEA, stimulator (STG1004), amplifier (MEA1060), temperature control units, data acquisition hardware (Mc_Card) and software (Mc_Rack). The MEA contained 64 circular-shaped electrodes in an 8×8 grid layout with electrode diameters of 30 μm and inter-electrode distances of 200 μm. The electrodes are coated with porous titanium nitride (TiN) to minimize electrical impedance. The four electrodes at the vertices were inactive. Multi-electrode recordings of the retinal activity were obtained from 60 electrode channels with a bandwidth ranging from 10 to 3000 Hz at a gain of 1200. The data sampling rate was 25 kHz/channel. From the raw waveform of retinal recording, retinal ganglion cell (RGC) spikes and local field potentials were isolated by using 100 Hz high-pass filter and 20 Hz low-pass filter respectively, since the *rd1* retina is known to have the oscillatory local field potential with ~10 Hz rhythm [9,26,27].

Electrical stimulation

Using a stimulus generator (STG 1004, Multichannel systems GmbH, Germany), current pulse trains were delivered to the retinal preparation via one of the 60 channels (mostly channel 44 in the middle of the MEA). The remaining channels of the MEA were used to record the responses of the RGCs (see Fig. 1B). The stimuli consisted of symmetric and asymmetric, anodic phase-1st biphasic pulses and cathodic phase-1st biphasic pulses (Fig. 1A). For the symmetric pulse, 1st and 2nd phase of pulse are exactly same amplitude and duration without any interphase delay. For the asymmetric pulse, 1st phase of the pulse is the same with symmetric pulse but the amplitude of 2nd phase of the pulse is less than 10 μA and charge balanced condition is satisfied by lengthening the pulse duration. Because we had previously found that 30 μA /500 μs stimuli evoked the most RGC spikes, we fixed pulse width at 500 μs for amplitude modulation and pulse amplitude at 30 μA for amplitude modulation. For amplitude modulation, the intensities of the pulse used ranged from 2 to 60 μA. For duration modulation, the pulse widths used ranged from 60 to 1000 μs. Biphasic current pulses were applied once per second (1 Hz, ×50 times).

### Calculation of threshold charge density

By using injected current, we can calculate the threshold charge density as follows when current stimuli were applied:

$$D = I \cdot T \ / \ \pi r^2 \qquad \text{(equation 1)}$$

Where D is the charge density, I is the injected current, T is the threshold duration of stimulation extracted by curve fitting (see details below - data analysis section), and r is the radius of the electrode (15 μm).

Threshold current and threshold charge density always refer to the 1st phase of the biphasic, charge-balanced stimulus pulse.

A. Stimulus Pulse Protocol
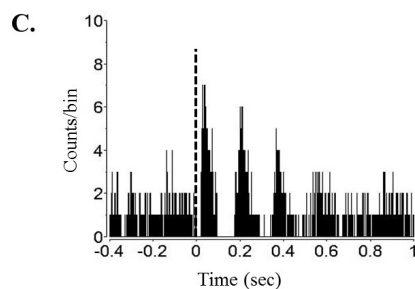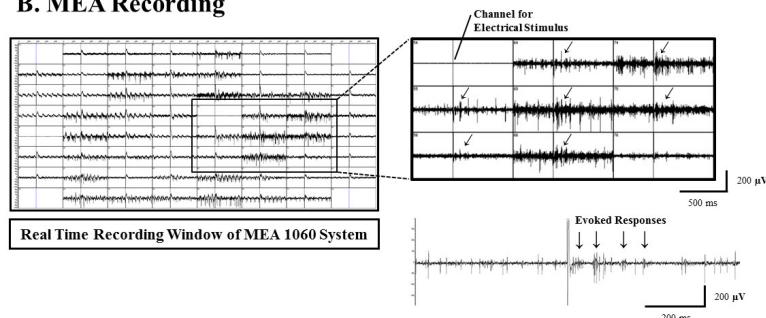

B. MEA Recording

C.
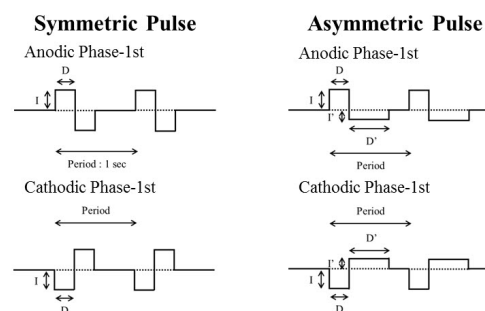
Fig. 1. Current pulse protocol for electrical stimulation, real time recording window of MEA1060 system and typical post-stimulus time histogram (PSTH) shape in *rd1* mice. (A) Pulse protocol for biphasic current stimulation. There is no interphase delay between the 1st and 2nd phase. The period is 1 second. For symmetric pulse protocol, charge of the 1st and 2nd phase is identical (I×D). For asymmetric pulse protocol, the 1st phase and 2nd phase has same charge (I×D=I'×D') but intensity (I') and duration (D') of the 2nd phase are different with those of 1st phase. The amplitude of 2nd phase pulse is set under 10 μA to minimize the membrane potential change. Pulse amplitude (I) and duration (D) were modulated. (B) Real time recording window of MEA 1060 system. Upper trace: Through channel 54, biphasic current pulses were applied, and retinal ganglion cell (RGC) spikes were recorded with all other channels. The oblique arrow (✓) at each channel of MEA represents the exact timing when the electrical stimulus was applied. Lower trace: Typical retinal waveforms recorded under electrical stimulation show that rhythmic burst-type firing of RGC spikes on top of background oscillatory rhythm of ~10 Hz. (C) PSTH constructed from 50 trials with pulse amplitude at 30 μA. This PSTH shows the typical temporal structure of an RGC spike train in *rd1* retina. Multiple peaks are present with interpeak intervals that were close to the interburst interval of spikes in lower trace of B (approximately 100 ms). The height of the first peak, occurring at approximately 70 ms, was much higher than those of later peaks, and the later peaks faded over poststimulus time. Typically, there were three or four peaks in 400 ms post stimulus time.

Data analysis

Stored data were processed off-line by the spike sorting software (Offline Sorter[TM], Plexon Inc., TX) to transform the waveforms containing multiunit activities into multiple single unit spike trains using principal component analysis (PCA) method [7,28-32]. From spike trains, all the data were processed with Neuroexplorer[TM] or Matlab[TM].

The temporal structure of RGC responses to electrical stimulus was investigated by Post-stimulus time histogram (PSTH), which shows multiple (3~4) peaks within 400 ms.

When there were 3 (or 4) distinctive peaks in the PSTHs, usually the number of spikes for post-stimulus 400 ms was 30% more than that for pre-stimulus 400 ms. Therefore, we identified RGC as response positive cell when above mentioned criteria were satisfied [11]. RGC response strength was quantified by counting the number of evoked RGC spikes per pulse, which is the difference between the number of spikes for post-stimulus 400 ms and pre-stimulus 400 ms.

The curves of RGC response versus current pulse amplitude or pulse duration were plotted. By curve fitting of RGC response curve with Boltzman equation,

$$y = \frac{A_1 - A_2}{1 + e^{(x-x_0)/dx}} + A_2 \qquad \text{(equation 2)}$$

We identified threshold amplitude or threshold duration when the number of evoked RGC spikes per pulse was 0.5. Fit quality was assessed by goodness of fit ($R^2 > 0.99$).

From the strength-duration curve, chronaxie and rheobase were calculated by fitting power functions $y = a/x + b$

[33,34]. The asymptote (coefficient b) was defined as rheobase; chronaxie was calculated as a/b. Fit quality was assessed by goodness of fit ($R^2 > 0.97$).

RESULTS

RGC responses were well modulated by both symmetric and asymmetric pulse protocols. In the symmetric pulse ex-

Table 1. The number of retinal patches and number of RGCs used for analysis

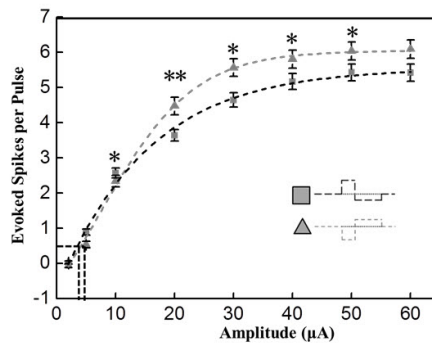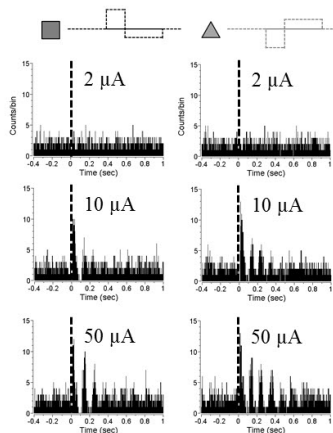|	Symmetric Pulse				Asymmetric Pulse			
	Amplitude Modulation		Duration Modulation		Amplitude Modulation		Duration Modulation	
	Anodic Phase-1st	Cathodic Phase-1st	Anodic Phase-1st	Cathodic Phase-1st	Anodic Phase-1st	Cathodic Phase-1st	Anodic Phase-1st	Cathodic Phase-1st
Number of Retina	11				6			
Number of RGC	225	162	194	153	135	175	135	148

Amplitude Modulation
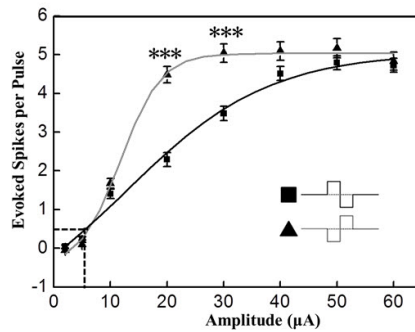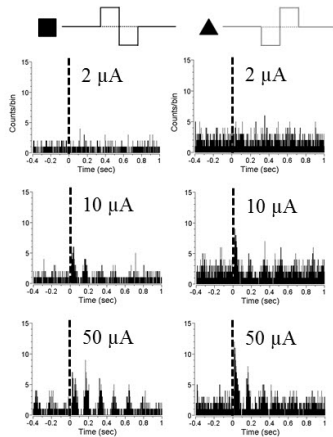
Fig. 2. Modulation of response strength based on pulse amplitude. Current pulse duration was fixed to 500 μs. (A) Amplitude modulation effect on evoked RGC spike number with symmetric pulse protocol. Left: Typical PSTH with different current amplitudes at 2, 10, and 30 μA. Right: Evoked RGC spike number versus current amplitude curve. Curves were fitted with Boltzmann equation. By curve fitting, the threshold amplitude is extracted as 6.36 μA, 7.12 μA for anodic phase, cathodic phase pulse, respectively. Cathodic phase-1st pulse is significantly efficient than anodic phase-1st pulse when the amplitude is 20, and 30 μA (***p < 0.001). (B) Amplitude modulation effect on evoked RGC spike number with asymmetric pulse protocol. Left: Typical PSTH with different current amplitudes at 2, 10, and 40 μA. Right: RGC response versus current amplitude curve. By curve fitting with Boltzmann function, the threshold amplitude is extracted as 3.57 μA, 4.28 μA for anodic, cathodic pulse, respectively. Cathodic phsase-1st pulse is significantly efficient than anodic phase-1st pulse at the amplitudes through 10~50 μA (*p < 0.05, **p < 0.01). Error bars denote SEM.

periments, we compared the average response of the retinas (n=11). For the analysis of amplitude modulation effect, 225 RGCs were used in the anodic phase-1st pulse and 162 RGCs were used in the cathodic phase-1st pulse. In duration modulation, 194 RGCs were used in the anodic phase-1st and 153 RGCs were used in the cathodic phase-1st pulse. In the asymmetric pulse experiments, we compared the average response of the retinas (n=6). 135 RGCs were used in the anodic phase-1st amplitude modulation and 175 RGCs were used in the cathodic phase-1st amplitude modulation. In duration modulation, 135 RGCs were used in the anodic phase-1st and 148 RGCs were used in the cathodic phase-1st pulse (Table 1). The usage of the terms cathodic or anodic, henceforth refer to the 1st phase of the biphasic, charge-balanced stimulus pulse.

Amplitude modulation

With amplitude increment, evoked RGC spike number increased both with symmetric and asymmetric pulse (Fig. 2). With the symmetric pulse protocol, cathodic pulses evoked significantly more RGC spikes than anodic pulses. At 20 and 30 μA amplitude there is a significant difference in evoked RGC spike numbers between cathodic and anodic pulse stimuli ($p < 0.001$).

With the asymmetric pulse protocol, cathodic pulses also evoked more RGC spikes than anodic pulses (between 10 to 50 μA: at 20 μA: $p < 0.01$, at other amplitudes: $p < 0.05$).
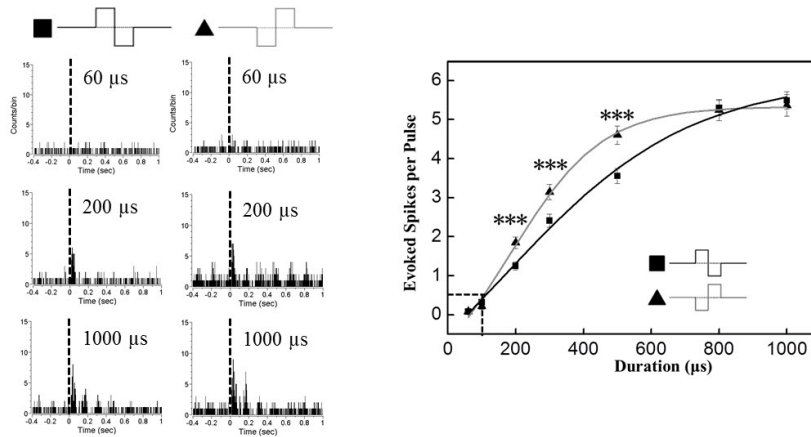
Duration modulation

Similar to the results from amplitude modulation, evoked RGC spike number increased with duration increment of both symmetric and asymmetric pulses (Fig. 3). With the symmetric pulse protocol, cathodic pulses evoked significantly more RGC spikes than anodic pulse at 200, 300, and 500 μs duration ($p < 0.001$).

With the asymmetric pulse protocol, cathodic pulses evoked significantly more RGC spikes from 100 to 500 μs (100 μs, 500 μs: $p < 0.05$; 200 μs, 300 μs: $p < 0.001$).
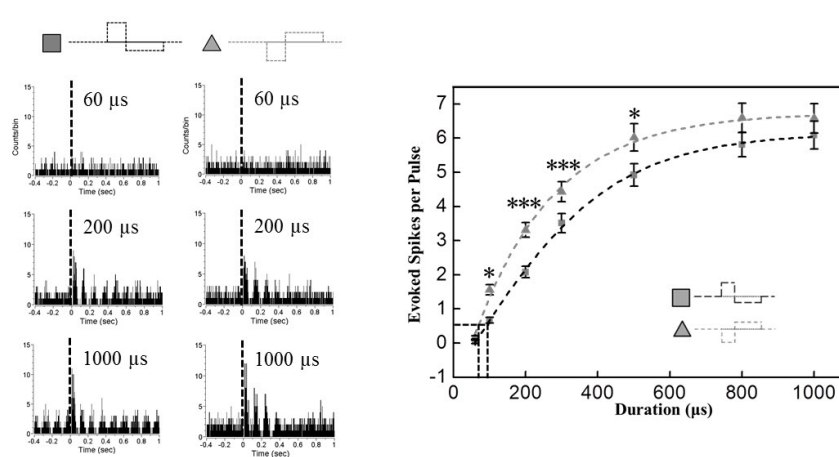
Duration Modulation

Fig. 3. Modulation of response strength based on pulse duration. Current pulse amplitude was fixed to 30 μA. (A) Duration modulation effect on evoked RGC spike number with symmetric pulse protocol. Left: Typical PSTH with different current durations at 60, 200, and 1000 μs. Right: RGC response versus current duration curve. By curve fitting with Boltzman function, the threshold duration is extracted as 114.80 μs, 115.96 μs for anodic, cathodic pulse, respectively. Cathodic phase-1st pulse is significantly efficient than anodic phase-1st pulse when the duration is 200, 300, and 500 μs (***$p < 0.001$). (B) Duration modulation effect on evoked RGC spike number with asymmetric pulse protocol. Left: Typical PSTH with different current duration at 60, 200, and 1000 μs. Right: RGC response versus current duration curve. By curve fitting with Boltzman function, the threshold duration is extracted as 89.54 μs, 70.16 μs for anodic, cathodic pulse, respectively. Cathodic phase-1st pulse is significantly efficient than anodic phase-1st pulse when the duration is 100, 200, 300, and 500 μs (*$p < 0.05$, ***$p < 0.001$). Error bars denote SEM.

Table 2. Threshold current and threshold charge density

Amplitude Modulation	Symmetric Pulse		Asymmetric Pulse	
	Anodic Phase-1st	Cathodic Phase-1st	Anodic Phase-1st	Cathodic Phase-1st
Threshold (μA)	(14.78±10.59***)†	7.83±3.71	4.77±3.58†	6.76±4.72
Charge Density (μC/cm^2)	1046±750	554.14±262.56	337.58±253.36	478.42±334.04

Duration Modulation	Symmetric Pulse		Asymmetric Pulse	
	Anodic Phase-1st	Cathodic Phase-1st	Anodic Phase-1st	Cathodic Phase-1st
Threshold (μs)	(241.95±177.99***)†	155.12±93.15†	124.67±69.69	101.33±71.89
Charge Density (μC/cm^2)	1027±750	656.68±395.54	529.38±295.92	430.28±305.27

Threshold was extracted by curve fitting of each RGC's modulationcurve. Mean±S.D. was shown. With symmetric anodic phase-1st pulse, the threshold current was significantly higher than other pulses (***p<0.001 with ANOVA). Statistically different groups were shown with posthoc Duncan criteria (†p<0.05).

Strength-Duration Curve

A. Symmetric Pulse
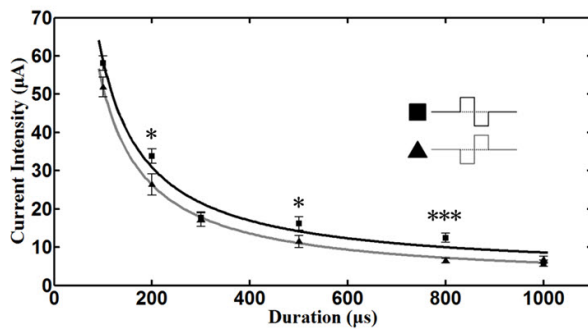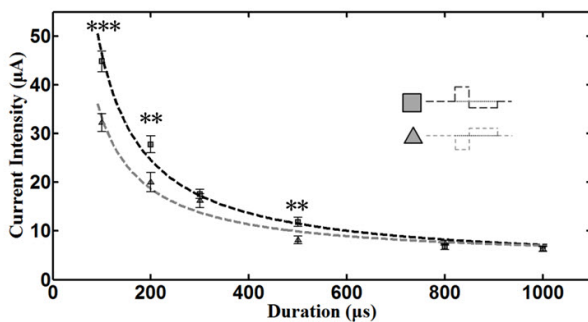

B. Asymmetric Pulse

Fig. 4. Strength-duration curve with current pulse. (A) With symmetric pulse, cathodic phase-1st pulse needs significantly lower amplitude of pulse than anodic phase-1st pulse when the duration is 200, 500 μs (*p<0.05), and 800 μs (***p<0.001). (B) With asymmetric pulse, cathodic phase-1st pulse needs significantly lower amplitude of pulse than anodic phase-1st pulse when the duration is 100 μs (***p<0.001), 200 and 600 μs (**p<0.01). Curves were fitted with power functions, and chronaxie and rheobase were extracted. Error bars denote SEM.

Threshold charge density

The calculated charge densities are summarized in Table 2. From each RGC modulation curve, we curve-fitted and extracted the threshold current. Then we calculated threshold charge density using equation 1. The mean±S.D. is shown under each pulse shape. Symmetric anodic pulses consistently exhibit the highest thresholds among different pulse shapes (***p<0.001 with ANOVA). With asymmetric pulses, anodic pulses exhibit lower thresholds than cathodic symmetric pulses for amplitude modulation.

Strength-Duration curve

The relationship between the strength of an applied current pulse required to initiate a spike and the duration of the pulse, known as the strength-duration curve is shown in Fig. 4. Higher currents were required to evoke a spike when shorter pulses were applied.

To characterize each strength-duration (SD) curve by a time constant and an asymptote, power functions were fit to our data. The current required to elicit a spike depended strongly on pulse duration. The threshold current decreases with increasing pulse duration. At very long pulse duration, the current is a minimum, called the rheobase. Rheobase is defined as the asymptote of the fit curve [35,36] and chronaxie, the classical measure of responsiveness of a neuron, as the duration at which the threshold current is twice the rheobase [34]. By using the power function of $y=a/x+b$, extracted rheobase was 0.89, 3.07, 4.10, 2.83 μA for symmetric cathodic, symmetric anodic, asymmetric cathodic, and asymmetric anodic pulse respectively. The chronaxie of each different pulse shape (above mentioned order) was 5.66, 1.81, 0.71, and 1.54 ms respectively. These results were obtained from 46 RGCs (2 retinal patches for each different pulse shape).

Our SD curves show that with anodic pulses, higher current is needed to elicit RGC spikes both in symmetric and asymmetric pulse stimuli.

DISCUSSION

Anodic phase-1st pulse vs. Cathodic phase-1st pulse

Cathodic (negative) pulses lower the potential of the medium near the electrode. Therefore, the proximal part of the cell soma including the axon hillock with its high density of sodium [37] is relatively depolarized, resulting lower threshold for generating spikes. On the other hand, with

Polarity effect of Current pulse on proximal part of cell soma
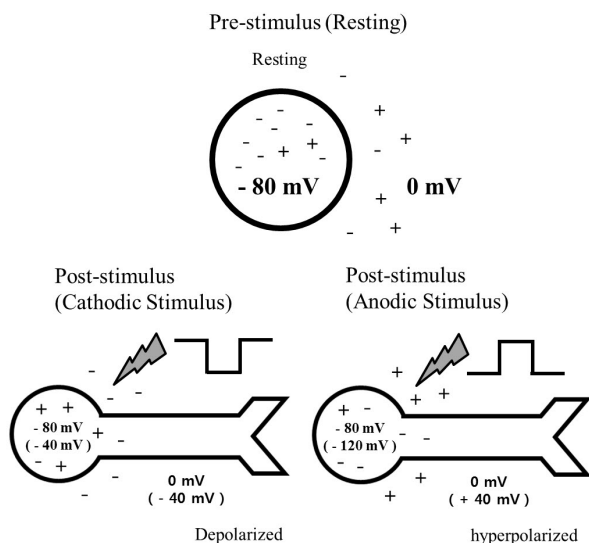
Pre-stimulus (Resting)

Fig. 5. Schematic diagram showing the effect of stimulus waveform of current pulse on proximal part of cell soma. When hyperpolarization from 0 mV to −40 mV occurs with a cathodic stimulus, proximal part of the cell soma including axonal hillock is depolarized from −80 mV to −40 mV, resulting in increased excitability. While depolarization from 0 mV to +40 mV occurs with an anodic pulse, the proximal part of the cell soma is hyperpolarized from −80 mV to −120 mV, resulting in decreased excitability.

anodic (positive) pulses the proximal part of the cell soma is relatively hyperpolarized. The schematic diagram (Fig. 5), illustrates the effect of switching stimulus waveform on the membrane potential of the proximal part of cell soma. Although the second phase of the pulse is needed for charge balance, it contributes little to activation of the cell since by the time of the second phase (0.2~1 ms), the RGC, having just fired a spike, is in a refractory state. Thus, only the effect of the first phase of the pulse on RGC firing is taken into consideration.

There are some reports showing that cathodic stimulation provides better result for eliciting RGC spikes. Jensen et al. [38] showed different response patterns with anodal and cathodal stimulation. Cathodal stimulation was associated with lower thresholds, making more localized stimulation possible. However, they used single needle platinum-iridium microelectrodes. Since we used planar disk microelectrode arrays, we are able to record the responses of several RGCs in the vicinity of stimulus channel, which is a major advantage of using MEA over single microelectrode. Moreover, since the configuration of MEA is similar to those used in current epiretinal prosthetics, we believe that our results are more applicable to retinal prostheses.

Using dissociated cerebral cortical neurons Wagenaar et al. [24] showed that pulse shape efficacy is best with biphasic negative then positive (equivalent to our biphasic cathodic phase-1st pulse).

Recently, Boinagrov et al. [39] also showed that cathodic epiretinal stimulation exhibit the lowest threshold for di-

rect RGC responses and the highest direct selectivity (network/direct thresholds ratio) with pulse durations below 0.5 ms. But for network-mediated stimulation, the lowest threshold was obtained with anodic pulses in the outer plexiform layer (OPL) position, and its network selectivity (direct/network thresholds ratio) increased with pulse duration.

Since we used multichannel recording with iridium oxide electrodes, after applying electrical stimulus through one channel (mostly channel number 44 in the center), we calculated the differences of spike numbers during 400 ms time period before and after the stimulus in each channel and we averaged evoked spike number throughout all the channels which satisfied the selection criteria (refer to method section). All our RGC response curves were drawn with average evoked spike number (Fig. 2). We extracted threshold current level by curve fitting when the evoked spike number per pulse was 0.5, which is a similar idea with typical threshold definition. Many groups define threshold current as the level when 50% of trial pulses evoke spikes at that level. We could not use typical threshold definition because big stimulus artifact obscured the short latency-direct RGC response within 10 ms. With different threshold definition, threshold charge density might be different in each different electrode setting [40], but all our calculated threshold charge densities were within 0.5 mC/cm^2, well within the safety limits of iridium oxide electrodes (1~4 mC/cm^2, [23]).

In our MEA experiments, asymmetric pulses with longer 2nd phase duration provided lower threshold irrespective of amplitude modulation or duration modulation (Fig. 3). This appears to be due to the fact that the larger stimulus artifacts in our MEA60 system make it more stable when the charge is balanced for longer time periods with asymmetric pulse.

Strength-Duration curve

Pulses significantly longer than chronaxie contribute little to the evoked spike, thus pulse durations smaller than chronaxie should be used to ensure that most of the applied charge contributes to evoking a response [41]. From our chronaxie values (5.66, 1.81, 0.71, and 1.54 ms), we suggest that optimal pulse duration should not exceed these values.

Because cell bodies and dendrites have chronaxies of 1-10 ms [33,36], we think cell bodies not the axons are most likely excited by electrical stimulus. The initial axon segment near the cell somas has exceptionally high density of sodium channels [42], the chronaxie for activation of axon should be lower.

Limitation of our study and future study

With electrical stimulation, the electrical signals applied to activate neurons are sensed by all electrodes of MEA as stimulus-related artifacts, with amplitudes several orders of magnitude large than the amplitudes of the recorded spikes. This can result in saturation of the recording amplifier and makes detection of the spike very difficult. The stimulus-related artifacts can be reduced by optimization of the stimulation circuitry [43,44] as well as by using artifact subtraction algorithm such as SALPA (subtraction of artifact by local polynomial approximation) during data analysis [40,45]. Since we are using commercially available MEA 64 systems, if we use the blank circuit for stimulus,

we lose recording for substantial time period (10^2 ms range) depending on stimulus amplitude. Therefore, we did not use blank circuit, resulting in large stimulus artifact. Due to the afore-mentioned technical reason, we have not dissected direct and indirect RGC responses, separately in this study.

The other limitation of our study is we did not consider spatial resolution. The RGC response curves we have shown in this study were drawn with averaged RGC spike number throughout all the channels with electrical stimulus. The MEA electrode we have been using has 200 μm inter-electrode distance. If we separate the channels with the distance from the stimulation channel, we can have preliminary data about spatial resolution with electrical stimulus.

A retinal prosthesis must be capable of delivering pulses and evoke spikes at a wide range of stimulation frequencies to mimic natural spike trains. Comparing the amplitude modulation and frequency modulation on percept size in RP patients with retinal prosthesis implanted, frequency modulation improves the encoding of a wide range of brightness levels without a loss of spatial resolution [46]. Since we have been using 1 Hz stimulus in this study, our next step will be frequency modulation.

ACKNOWLEDGEMENTS

REFERENCES

1. **Arnold JJ, Heriot W.** Age related macular degeneration. *Clin Evid (Online).* 2007;2007. pii: 0701.
2. **Sieving PA, Caruso RC.** Retinitis pigmentosa and related disorders. In: Yanoff M, Duker JS, editors. Ophthalmology. 3rd ed. Maryland Heights: Elsevier; 2008. chap 6.10.
3. **Chader GJ, Weiland J, Humayun MS.** Artificial vision: needs, functioning, and testing of a retinal electronic prosthesis. *Prog Brain Res.* 2009;175:317-332.
4. **Rizzo JF 3rd.** Update on retinal prosthetic research: the Boston Retinal Implant Project. *J Neuroophthalmol.* 2011;31:160-168.
5. **Zrenner E, Bartz-Schmidt KU, Benav H, Besch D, Bruckmann A, Gabel VP, Gekeler F, Greppmaier U, Harscher A, Kibbel S, Koch J, Kusnyerik A, Peters T, Stingl K, Sachs H, Stett A, Szurman P, Wilhelm B, Wilke R.** Subretinal electronic chips allow blind patients to read letters and combine them to words. *Proc Biol Sci.* 2011;278:1489-1497.
6. **Tombran-Tink J, Barnstable CJ, Rizzo JF 3rd.** Visual prosthesis and ophthalmic devices: new hope in sight. Totawa: Humana Press; 2007.
7. **Grumet AE, Wyatt JL Jr, Rizzo JF 3rd.** Multi-electrode stimulation and recording in the isolated retina. *J Neurosci Methods.* 2000;101:31-42.
8. **Stett A, Barth W, Weiss S, Haemmerle H, Zrenner E.** Electrical multisite stimulation of the isolated chicken retina. *Vision Res.* 2000;40:1785-1795.
9. **Ye JH, Goo YS.** The slow wave component of retinal activity in rd/rd mice recorded with a multi-electrode array. *Physiol Meas.* 2007;28:1079-1088.
10. **Ye JH, Ryu SB, Kim KH, Goo YS.** Functional connectivity map of retinal ganglion cells for retinal prosthesis. *Korean J Physiol Pharmacol.* 2008;12:307-314.
11. **Goo YS, Ye JH, Lee S, Nam Y, Ryu SB, Kim KH.** Retinal ganglion cell responses to voltage and current stimulation in wild-type and rd1 mouse retinas. *J Neural Eng.* 2011;8:035003.
12. **Goo YS, Ahn KN, Song YJ, Ahn SH, Han SK, Ryu SB, Kim KH.** Spontaneous oscillatory rhythm in retinal activities of two retinal degeneration (rd1 and rd10) mice. *Korean J Physiol Pharmacol.* 2011;15:415-422.
13. **Jae SA, Ahn KN, Kim JY, Seo JH, Kim HK, Goo YS.** Electrophysiological and histologic evaluation of the time course of retinal degeneration in the rd10 mouse model of retinitis pigmentosa. *Korean J Physiol Pharmacol.* 2013;17:229-235.
14. **Liu W, Vichienchom K, Clements M, DeMarco SC, Hughes C, McGucken E, Humayun MS, de Juan E, Weiland JD, Grenberg R.** A neuro-stimulus chip with telemetry unit for retinal prosthetic device. *IEEE Journal of Solid-State Circuits.* 2000;35:1487-1497.
15. **Brummer SB, Turner MJ.** Electrical stimulation of the nervous system:the principle of safe charge injection with noble metal electrodes. *Bioelectrochem Bioenerg.* 1975;2:13-25.
16. **Lilly JC, Hughes JR, Alvord EC Jr, Galkin TW.** Brief, noninjurious electric waveform for stimulation of the brain. *Science.* 1955;121:468-469.
17. **Mortimer JT, Shealy CN, Wheeler C.** Experimental non-destructive electrical stimulation of the brain and spinal cord. *J Neurosurg.* 1970;32:553-559.
18. **Mortimer JT, Kaufman D, Roessman U.** Intramuscular electrical stimulation: tissue damage. *Ann Biomed Eng.* 1980;8:235-244.
19. **Scheiner A, Mortimer JT, Roessmann U.** Imbalanced biphasic electrical stimulation: muscle tissue damage. *Ann Biomed Eng.* 1990;18:407-425.
20. **Shepherd RK, Javel E.** Electrical stimulation of the auditory nerve: II. Effect of stimulus waveshape on single fibre response properties. *Hear Res.* 1999;130:171-188.
21. **Merrill DR, Bikson M, Jefferys JG.** Electrical stimulation of excitable tissue: design of efficacious and safe protocols. *J Neurosci Methods.* 2005;141:171-198.
22. **Wagenaar DA, Pine J, Potter SM.** Effective parameters for stimulation of dissociated cultures using multi-electrode arrays. *J Neurosci Methods.* 2004;138:27-37.
23. **Farber DB, Flannery JG, Bowes-Rickman C.** The rd mouse story: seventy years of research on an animal model of inherited retinal degeneration. *Prog Ret Eye Res.* 1994;13:31-64.
24. **McLaughlin ME, Sandberg MA, Berson EL, Dryja TP.** Recessive mutations in the gene encoding the beta-subunit of rod phosphodiesterase in patients with retinitis pigmentosa. *Nat Genet.* 1993;4:130-134.
25. **McLaughlin ME, Ehrhart TL, Berson EL, Dryja TP.** Mutation spectrum of the gene encoding the beta subunit of rod phosphodiesterase among patients with autosomal recessive retinitis pigmentosa. *Proc Natl Acad Sci U S A.* 1995;92:3249-3253.
26. **Margolis DJ, Newkirk G, Euler T, Detwiler PB.** Functional stability of retinal ganglion cells after degeneration-induced changes in synaptic input. *J Neurosci.* 2008;28:6526-6536.
27. **Menzler J, Zeck G.** Network oscillations in rod-degenerated mouse retinas. *J Neurosci.* 2011;31:2280-2291.
28. **Nicolelis MAL.** Methods for neural ensemble recordings. New York: CRC press; 1999.
29. **Meister M, Berry MJ 2nd.** The neural code of the retina. *Neuron.* 1999;22:435-450.
30. **Jin GH, Cho HS, Lee TS, Goo YS.** PCA-based waveform classification of rabbit retinal ganglion cell activity. *Korean J Medical Physics.* 2003;14:211-217.
31. **Chapin JK, Nicolelis MA.** Principal component analysis of neuronal ensemble activity reveals multidimensional somatosensory representations. *J Neurosci Methods.* 1999;94:121-140.
32. **Jolliffe IT.** Principal component analysis. New York: Springer-Verlag; 2005.
33. **Holsheimer J, Demeulemeester H, Nuttin B, de Sutter P.** Identification of the target neuronal elements in electrical deep brain stimulation. *Eur J Neurosci.* 2000;12:4573-4577.
34. **Lapicque L.** Recherches quantitatives sur l'excitation electrique des nerfs traites comme un polarization. *J Physiol Paris.* 1907;9:620-635.

35. **Loeb GE, White MW, Jenkins WM.** Biophysical considerations in electrical stimulation of the auditory nervous system. *Ann N Y Acad Sci.* 1983;405:123-136.

36. **Ranck JB Jr.** Which elements are excited in electrical stimulation of mammalian central nervous system: a review. *Brain Res.* 1975;98:417-440.

37. **Fried SI, Lasker AC, Desai NJ, Eddington DK, Rizzo JF 3rd.** Axonal sodium-channel bands shape the response to electric stimulation in retinal ganglion cells. *J Neurophysiol.* 2009;101: 1972-1987.

38. **Jensen RJ, Rizzo JF 3rd, Ziv OR, Grumet A, Wyatt J.** Thresholds for activation of rabbit retinal ganglion cells with an ultrafine, extracellular microelectrode. *Invest Ophthalmol Vis Sci.* 2003;44:3533-3543.

39. **Boinagrov D, Pangratz-Fuehrer S, Goetz G, Palanker D.** Selectivity of direct and network-mediated stimulation of the retinal ganglion cells with epi-, sub- and intraretinal electrodes. *J Neural Eng.* 2014;11:026008.

40. **Sekirnjak C, Hottowy P, Sher A, Dabrowski W, Litke AM, Chichilnisky EJ.** Electrical stimulation of mammalian retinal ganglion cells with multielectrode arrays. *J Neurophysiol.* 2006;95:3311-3327.

41. **Tehovnik EJ.** Electrical stimulation of neural tissue to evoke behavioral responses. *J Neurosci Methods.* 1996;65:1-17.

42. **Wollner DA, Catterall WA.** Localization of sodium channels in axon hillocks and initial segments of retinal ganglion cells. *Proc Natl Acad Sci U S A.* 1986;83:8424-8428.

43. **Jimbo Y, Kawana A.** Electrical stimulation and recording from cultured neurons using a planar electrode array. *Bioelectrochem Bioenerg.* 1992;29:193-204.

44. **Brown EA, Ross JD, Blum RA, Yoonkey Nam, Wheeler BC, Deweerth SP.** Stimulus-artifact elimination in a multi-electrode system. *IEEE Trans Biomed Circuits Syst.* 2008;2:10-21.

45. **Wagenaar DA, Potter SM.** Real-time multi-channel stimulus artifact suppression by local curve fitting. *J Neurosci Methods.* 2002;120:113-120.

46. **Nanduri D, Fine I, Horsager A, Boynton GM, Humayun MS, Greenberg RJ, Weiland JD.** Frequency and amplitude modulation have different effects on the percepts elicited by retinal stimulation. *Invest Ophthalmol Vis Sci.* 2012;53:205-214.